THE JOURNAL OF PHYSICAL CHEMISTRY B

ARTICLE

pubs.acs.org/JPCB

Matrix and Polymer Soft-Landing Isolation of Selected Acids with Pyridine and Poly(4-vinylpyridine): A Comparative Infrared Spectroscopic Study of Hydrogen Bonding

Alejo M. Lifschitz, Jeffrey M. Rodgers, and Cindy Samet*

Department of Chemistry, Dickinson College, Carlisle, Pennsylvania 17013, United States

Supporting Information

ABSTRACT: Hydrogen bonding plays a key role in the formation of nanostructures, as it is the "glue" between layers that are built by the layer-by-layer technique. Poly (4-vinylpyridine) (PVP) is one of the most commonly used polymers in these sandwich-structured films, often in conjunction with poly(carboxylic acid)s such as poly(acrylic acid) in the PVP/PAA interpolymer complex. In addition, PVP is commonly used as a polymer matrix for embedding semiconductor nanoparticles. In this study, hydrogen-bonded complexes of water, formic acid, and pentachlorocyclopropane, with pyridine in a traditional matrix isolation experiment and PVP in a novel "polymer soft-landing" isolation experiment, have been characterized for the first time at 16 K. Changes in vibrational modes of the proton donor species and in some cases pyridine modes provided ample evidence for complex formation. In the case of water and pentachlorocyclopropane, the matrix and polymer soft-landing results were quite similar, whereas formic acid formed a significantly different complex with pyridine in the argon matrix than with the pyridine ring on the PVP polymer. This work demonstrates clearly the benefit of using both the conventional matrix isolation technique and our polymer soft-landing variation in tandem to probe the structure of these complexes and thus elucidate the nature of the C−H···N, C−H···O═C, and O−H···N linkages.

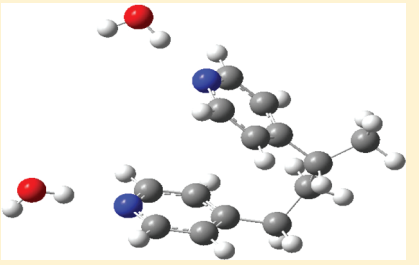

INTRODUCTION

Hydrogen bonds are weak chemical bonds that play a key role in both the natural and synthetic worlds. In nature, they represent an interaction, both fundamental and diverse, capable of determining the structure of biomolecules ranging from deoxyribonucleic acid (DNA), the carrier of genetic information in cells, to spider silk, the strength of which exceeds that of steel. Synthetically, hydrogen bonds have played a key role in crystal engineering,[1] cluster-based organometallic chemistry,[2] and macrocyclization processes,[3] to name but a few examples. More recently, hydrogen bonding has become an important driving force in the formation of nanostructures.[4,5] In the world of nanofabrication, two synthetic approaches exist: "top-down" methods in which one starts at the macroscopic level and carves out something small (such as in nanolithography), and "bottom-up" techniques in which the final structure is built by manipulating atoms and molecules. In a bottom-up method known as *layer by layer (LbL) assembly*, thin films containing nanoparticles are organized in sandwich-like layers that may be held together by a variety of covalent and noncovalent interactions.[4] The LbL assembly through hydrogen bonding, first demonstrated in 1997 by Rubner et al.,[5] is one of the most versatile LbL assembly strategies because of the vast number of available hydrogen-acceptor and hydrogen-donor species.

The matrix isolation technique, both in its traditional and modified "polymer soft-landing" form, is ideal for the study of hydrogen bonding and thus has the potential to yield valuable information about linkages found to be important in the building of nanostructures. In a traditional matrix isolation experiment, the "guest" molecules are diluted with a rare gas "host" (usually argon) and then codeposited onto a cold surface. In our "polymer soft-landing isolation" experiment, a "guest" species, diluted in argon, is deposited onto a cold surface that has been coated with a polymer. Thus, our version of the soft-landing technique represents just a small modification to the existing matrix isolation technique in that the second species (diluted with argon) that would be deposited onto the cold surface is now replaced with a polymer. Although this new variation of the matrix isolation technique, which we refer to as "polymer soft-landing", is quite different from the "soft-landing" technique reported in the literature[6] we retained the term "soft- landing" in the name for our new technique, because we are also depositing isolated guest species onto a solid support. In the typical soft-landing experiments reported in the literature,[6] gas-phase ions are deposited at low energies (collision energy of about 20 eV) onto either a solid substrate such as gold or any bare metal, a metal surface covered with a low temperature Ar matrix to "soften" the landing and serve as a buffer, or a self-assembled monolayer.[6] In our version of the technique, neutral molecules are deposited onto a polymer-coated CaF_2 surface. Furthermore, we matched the functional

Received: August 19, 2011
Revised: November 21, 2011
Published: November 23, 2011

group on the polymer (a pyridine ring) with the base species (pyridine/argon) in the traditional matrix isolation experiment to provide evidence for the formation of hydrogen-bonded product *and* to study the matrix and polymer soft-landing methods in a comparative way. In either matrix or polymer soft-landing isolation, hydrogen bond formation manifests itself as a distinct shift, broadening, and intensification of the proton donor stretching and bending modes in the infrared spectrum. We note that when discussing our current work, we will simply use the term soft-landing to refer to our version of the soft-landing technique (i.e., polymer soft-landing).

The work in our laboratory has focused on nonconventional C−H···N and C−H···O hydrogen bonds, ranging from the very weakly bound bromocyclopropane−NH_3 complex with hydrogen bond strength of 2.35 kcal/mol (MP2),[7] to the more strongly bound pentachlorocyclopropane−dimethylamine complex with hydrogen bond strength of 4.2 kcal/mol (B3LYP).[8] This study builds on our previous work while also serving to explore ways of using the matrix isolation laboratory to monitor the building of nanostructures and to understand, on a fundamental level, the interaction between layers in the interpolymer complexes built by the LbL method. In particular, three model molecules were chosen to compare the information obtained in matrix isolation and soft-landing isolation experiments. Specifically, pentachlorocyclopropane (Pccp), formic acid (FA), and water (H_2O) were codeposited with pyridine (Pyr) in a traditional matrix isolation experiment (with the exception of water which was already reported in the literature[9]) *and* deposited with argon onto a poly(4-vinylpyridine) (PVP) surface in a soft-landing isolation experiment. The pyridine functional group was chosen because, as a base, pyridine complements the other nitrogen bases studied in our laboratory and also serves as the isolated analogue for the PVP thin film, which has been referred to as a "universal surface modifier" for the immobilization of nanoparticles.[10] The PVP polymer is ideal for these studies because of its ability to hydrogen-bond with the "acids" (polar species) chosen and for its possible future use in our laboratory for studies in which we might bind metals to the pyridyl groups. Furthermore, we aimed to select acids that have been studied previously. Pccp has been well characterized in our laboratory with a range of bases;[8] FTIR studies of matrix-isolated Pyr−water complexes have already been published;[9] and FA, although not previously matrix-isolated with Pyr, has been extensively studied in argon matrixes,[11,12] and a theoretical study on FA−Pyr complexes has been reported.[13] Most important, the hydrogen bonds presented here (C−H···N, O−H···N, and C−H···O═C) are those that would be advantageous for building multilayer thin films. For example, the PVP/PAA (polyacrylic acid) thin film built by the LbL method, is composed of layers that form when the carboxylic acid groups of PAA hydrogen-bond to the pyridyl groups of PVP.[14] Despite the extensive use of this thin film *and* some detailed experimental studies, the nature of the interaction between carboxylic acids and pyridine is not well understood.[13]

Finally, to our knowledge, depositing isolated gas-phase molecules onto a polymer surface such as PVP at low temperatures has never been done, and in addition, few thin film or polymer studies have employed FTIR absorption spectroscopy alone (without reflection or attenuated reflection) to study the resulting complexes. We therefore thought the merging of the soft-landing technique with a polymer that is already very important in the building of nanostructures was worth investigating, and we see this work as an exciting first step into using the matrix isolation laboratory to probe the building of nanostructures. Moreover, the goal of these initial studies is not to provide a detailed structural analysis of the molecules themselves but rather to demonstrate the importance of both techniques *together* to yield valuable information to those building nanostructures.

EXPERIMENTAL METHODS

Matrix isolation and soft-landing isolation experiments were carried out in a completely stainless steel vacuum system, with Nupro Teflon-seat high vacuum valves. Pumping was provided by a Model 1400B Welch vacuum pump, and a turbomolecular pump (Varian V301). Pressures on the order of 10^{-7} mm Hg at the gauge (cold cathode, Varian) were attained using this apparatus. Cryogenics were supplied by a Model 22 closed cycle helium refrigerator (CTI Cryogenics, Inc.), which operates down to 10 K. Gas samples were deposited from 2-L stainless steel vessels through a precise metering valve onto the cold surface, which is a CsI window (for matrix experiments) or a CaF_2 window (for soft-landing experiments) mounted with indium gaskets to a copper block which is in turn mounted with indium gaskets on the second stage of the CTI Cryogenics refrigerator's cold head. Deposition of the gas samples was perpendicular to the cold surface. Temperatures at the second stage of the cold head were controlled and monitored by a LakeShore 321 digital cryogenic temperature controller. The vacuum vessel was equipped with CsI windows and sat in the sample beam of a Nicolet Nexus 670 infrared spectrometer for the duration of the experiment, and the sample was monitored during the entire deposition. The matrix isolation apparatus described here is standard and has been described thoroughly elsewhere in the literature.[15]

The liquid reagents employed were H_2O (house water, triply distilled), FA (Acros, 98+%), Pccp (Acros, 98%), and anhydrous Pyr (Acros, stored over molecular sieves, 99.8%). The FA was dried using boric anhydride and distilled at 101 °C.[16] Pccp was used without further purification. These reagents were subjected to one or more freeze−thaw cycles at 77 K prior to sample preparation. Argon (Matheson, 99.999%) was used without further purification as the matrix gas in all experiments. H_2O, FA, and Pyr samples were prepared by standard manomeric techniques in which the vapor is added to the vessel with the argon. Because Pccp is relatively involatile, we attached a side arm to the deposition line, separated by a valve. The argon then entrained the Pccp vapor from the side arm. This technique is commonly used with samples whose vapor pressure is less than 1 mmHg at room temperature. The drawback to such a technique is that it is difficult to vary and measure matrix ratios. Samples were deposited at rates of approximately 0.5−2 mmol/h, for times ranging from 18 to 24 h for matrix experiments and 1 min to 6 h for soft-landing experiments, and at temperatures ranging from 10 to 20 K. Survey scans and high-resolution scans were recorded at resolutions of 0.5, 0.25, and 0.125 cm^{-1}. Some samples were annealed to approximately 32 K, cooled to 16 K, and additional spectra were obtained.

For the soft-landing isolation experiments, a 1% w/v solution of PVP (typical M_w = 160 000, Sigma-Aldrich) was prepared in ethanol (200 proof). The thin film was placed on a clean, dry, CaF_2 deposition window by slowly adding 1% PVP solution with a pipet until a raised droplet covered the surface. We observed no difference in film quality whether the CaF_2 surface was treated

with a sulfuric acid and hydrogen peroxide mix (Piranha solution) or simply cleaned with acetone and carefully dried. As the solvent evaporated, the polymer was left as a translucent film. This process was attempted and modified multiple times to achieve the desired film; initial attempts were unsuccessful when the droplet size was too small, resulting in an opaque film. A 1% solution resulted in the desired thickness and translucency, and increasing the concentration did not result in more available hydrogen bonding sites. This value is consistent with Malynych et al. who reported that the PVP surface morphology is not dependent on concentration between 0.01 and 3%.[10]

Parent matrix and soft-landing isolation experiments were carried out in the single-jet mode, in which the samples were diluted with argon and deposited from a single vacuum line. The main difference between these two types of experiments is that in the matrix experiments, gaseous samples are deposited onto a CsI or KBr surface while in the soft-landing experiments they are deposited onto a PVP film that was put onto the CaF_2 window at room temperature. For the matrix codeposition experiments, the twin-jet method, in which the two reactants flowed from separate vacuum lines, was employed.

COMPUTATIONAL METHODS

Computations were carried out using the Gaussian 03 suite for Mac OS X to confirm complex assignments.[17] The B3LYP and BPW91 density functional methods were used for all calculations, and the electronic density of all atoms was represented by a 6-31+G(d, p) all-electron basis set. Geometries were fully relaxed during optimization, and initial starting orientations were given such that the CH···N (or OH···N) angle was nearly collinear. The interaction energy was computed as $\Delta E_{int} = E_{complex} - (E_{acid} + E_{base})$. Vibrational frequencies were calculated analytically from second derivatives of the potential surface, and all energy values reported include zero-point energy corrections. To evaluate hydrogen-bond interaction energies, basis set superposition error was corrected by the counterpoise method. We note that PVP films were modeled by optimizing the geometry of a 4-vinylpyridine monomer and repeating the unit through space twice. Hydrogen-bonding between the polymer and acid was studied by manually modeling a 4-vinylpyridine dimer and aligning a hydrogen-bonding molecule over the lone pair of electrons on the pyridine nitrogen.

RESULTS

Prior to any codeposition and soft-landing studies, blank experiments were carried out on the parent molecules, FA, H_2O, Pccp, Pyr, and PVP. The resulting spectra were in excellent agreement with literature spectra for FA,[11] H_2O,[9] Pccp,[8] Pyr,[9] and PVP.[14,18] Representative spectra, all recorded at 0.5 cm^{-1}, are shown in Figures 1−9. Results not shown as spectra are listed in Table 1.

H_2O + PVP. When $Ar/H_2O = 200$ was deposited onto a single layer 1% PVP film for 6 h, two new absorptions, associated with parent vibrations of H_2O, were observed at 3443.4 and 1612.3 cm^{-1} (see Figures 1 and 2). We note that parent dimer and trimer bands for H_2O were not shifted at all. Additionally, two significant new product absorptions associated with the pyridine ring modes of the PVP were observed at 2929.4 and 1259.1 cm^{-1}. We note that we did not perform Ar/H_2O/Pyr matrix isolation experiments but rather rely on the experimental results of Destexhe and co-workers.[9]

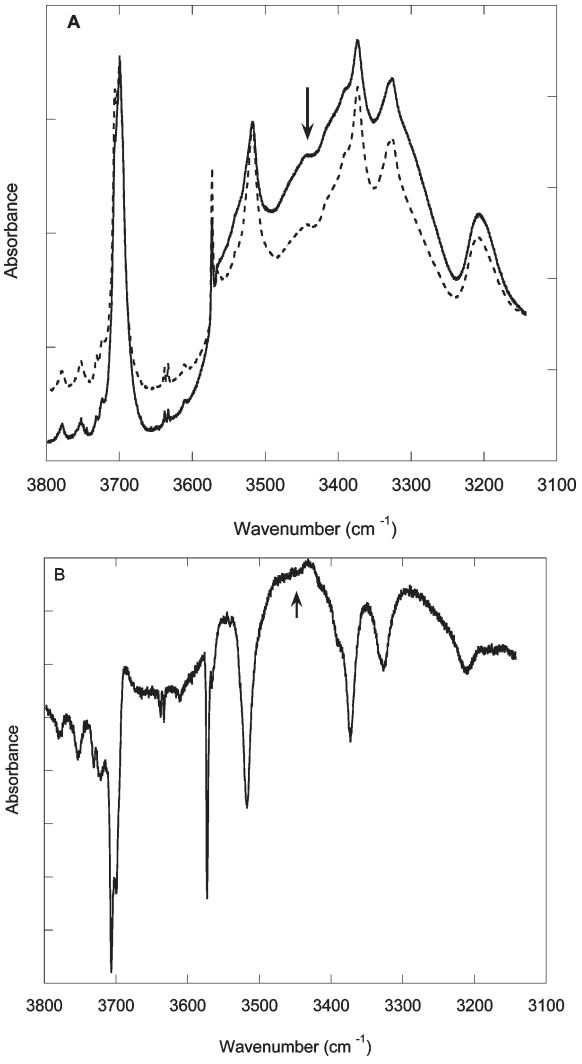

Figure 1. Infrared spectra in the region of water's symmetric and antisymmetric O−H stretches. Panel A shows parent $Ar/H_2O = 200$ (dash line) and $Ar/H_2O = 200$ soft-landed on PVP (solid line) at 16 K. The new product absorption is marked with an arrow. Panel B is the result of subtraction of Ar/H_2O from Ar/H_2O on PVP.

Pccp + Pyr. The codeposition of Pccp (unrestricted, being entrained by Ar, as in our previous work) with Ar/Pyr = 250 gave rise to many new infrared absorptions that were not present in the spectra of the individual parents. Most notably, a new product band at 2938.0 cm^{-1} appeared to the red of the parent CH stretch at 3044.5 cm^{-1}, and a small shoulder on this parent band was also observed (Figure 3). Additional significant new absorptions are summarized in Table 1, and we also note that these results, along with some changes in base modes, are strikingly similar to our previously published results (see Figure S1 of Supporting Information).

Pccp + PVP. When Ar/Pccp was deposited onto a single layer 1% PVP film, many new absorptions were observed. In particular, a broad, weak absorption appeared at 2939.9 cm^{-1}, to the red of the parent CH stretch, which itself shifted very slightly to 3045.5 cm^{-1} (Figure 3), and a small shoulder on this parent band was observed. Additional significant product bands are summarized in Table 1.

FA + Pyr. FA and Pyr were codeposited in many experiments at concentrations ranging from Ar/FA = 1000 to Ar/FA = 250

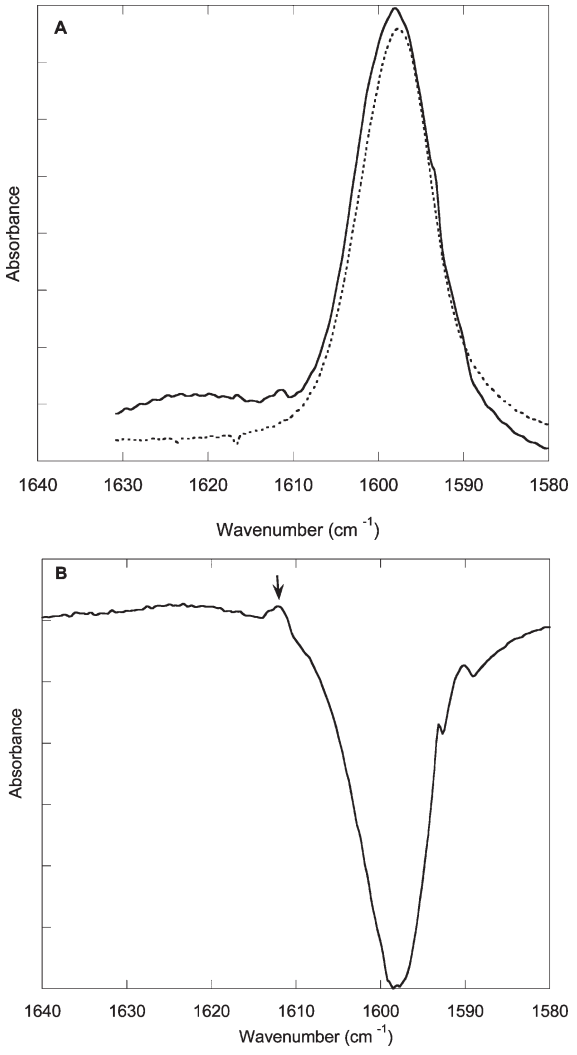

Figure 2. Infrared spectra in the region of water's H−O−H bend. Panel A shows parent Ar/H_2O = 200 (dash line) and Ar/H_2O = 200 soft-landed on PVP (solid line) at 16 K. Panel B shows the result of subtraction of Ar/H_2O from Ar/H_2O on PVP, and the product band is marked with an arrow.

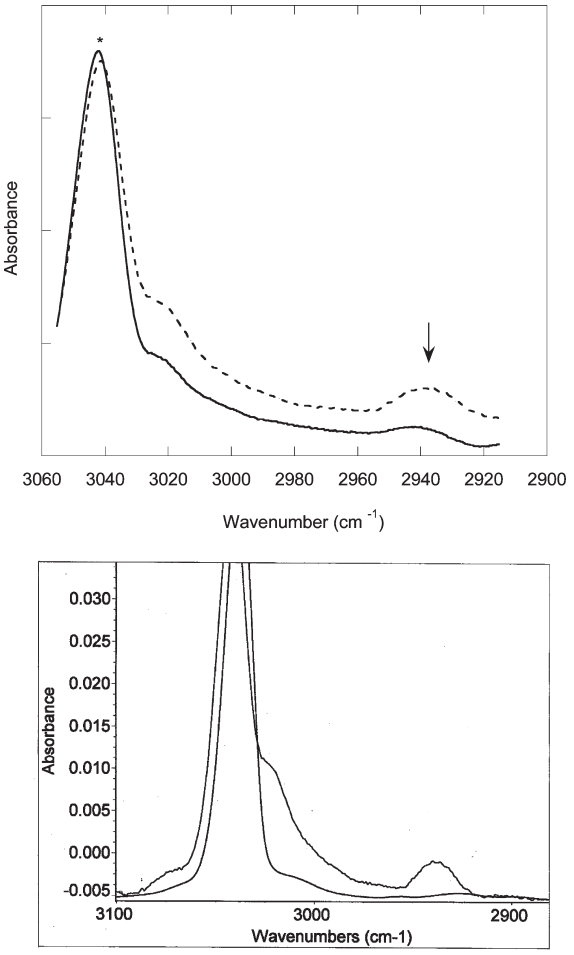

Figure 3. Infrared spectra in the C−H stretching region of Pccp. The upper panel shows Ar/Pccp (with Pccp unrestricted) soft-landed on PVP (solid line) and the codeposition of Ar/Pccp with Ar/Pyr = 250 in a traditional matrix isolation experiment (dash line). The new product absorption is marked with an arrow. The only parent band in the region is that of Pccp, marked with an asterisk. The lower panel shows parent Ar/Pccp on CaF_2 (bottom trace) and Ar/Pccp soft-landed on PVP (top trace) with a scale that allows the new product band at 2939.9 cm^{-1} to be seen clearly.

and Ar/Pyr = 500 to Ar/Pyr = 250. The codeposition spectra in which product bands were most easily observed occurred at FA/Pyr/Ar = 1/2/1000 and after annealing the sample to 32 K for 20 min and then cooling back down to 16 K. Three new product absorptions appeared at 2902.3, 1707.4, and 1203.4 cm^{-1}, associated with shifts in the three main formic acid parents stretches, namely the O−H, C═O, and C−O, respectively (Figures 4−6). In addition, three closely spaced product bands (3138.6, 3041.5, and 3006.5 cm^{-1}), broadened and blue-shifted from parent pyridine modes, were observed (Figure 4). These results are summarized in Table 1.

FA + PVP. Numerous experiments were conducted with concentrations ranging from Ar/FA = 1000 to Ar/FA = 250 in order to determine the most efficient ratio to maximize product formation and use all of the hydrogen bonding sites available on the PVP while simultaneously ensuring that FA clusters did not dominate the spectrum. Samples that were too dilute resulted in the Ar gas covering the surface and thus minimal formation of hydrogen-bonded product. When Ar/FA = 250 was deposited onto a single layer 1% PVP film for ∼6 h, several new absorptions were noted and more clearly observed upon subtraction of both FA and PVP parent spectra. In particular, a new, broad absorption was noted at 3095.7 cm^{-1} (Figure 7), along with a second new absorption at 1744.4 cm^{-1} (distinct from nearby dimer C═O stretches, see Figure 8) and a third at 1229.1 cm^{-1} (Figure 9). Upon annealing, parent bands grew and became more distinct (see Figure S3 in Supporting Information, for example). We note that there were no changes in the PVP (base) modes, and thus the PVP film was included in the background spectrum and subtracted from all spectra reported in Figures 7−9.

RESULTS OF CALCULATIONS

The chemical properties indicating the strength of the hydrogen bond (bond energy, bond lengths, and bond angles) as well as the vibrational frequencies for two of the three systems studied were calculated at the (B3LYP/6-31+G(d, p)) level. Because extremely in-depth theoretical studies of both H_2O−Pyr and

dx.doi.org/10.1021/jp2080012 |J. Phys. Chem. B 2012, 116, 211–220

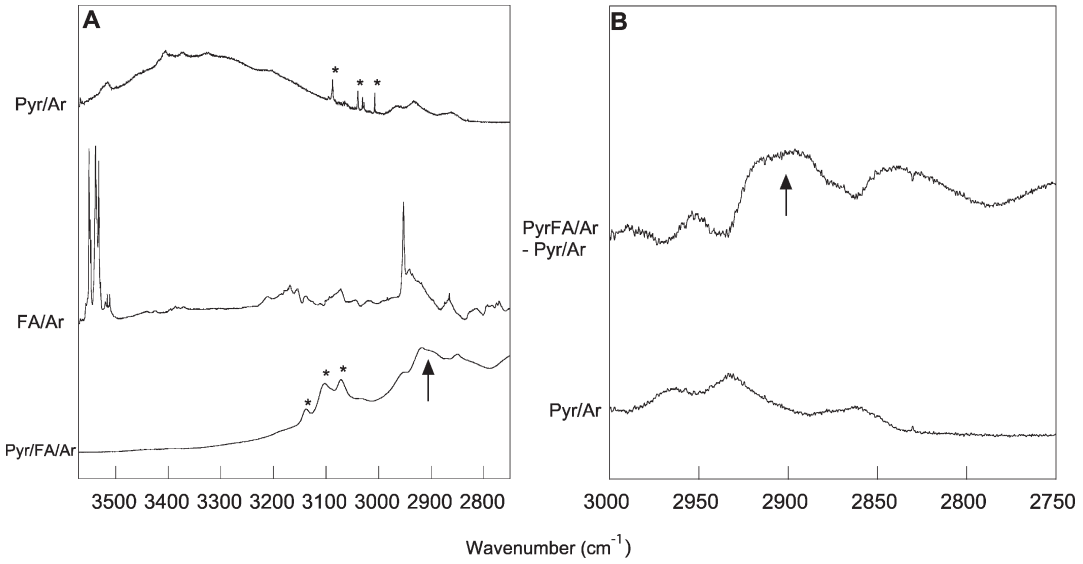

Figure 4. Infrared spectra in the O−H stretching region of FA and the C−H stretching region of Pyr in a traditional matrix isolation experiment at 16 K (after annealing) with FA/Pyr/Ar = 1/2/1000. Panel A shows parents and codeposition products (asterisks indicate Pyr C−H stretching modes, and the new product absorption is marked with an arrow.) Panel B shows the result of subtraction of parent Ar/Pyr from Ar/FA/Pyr.

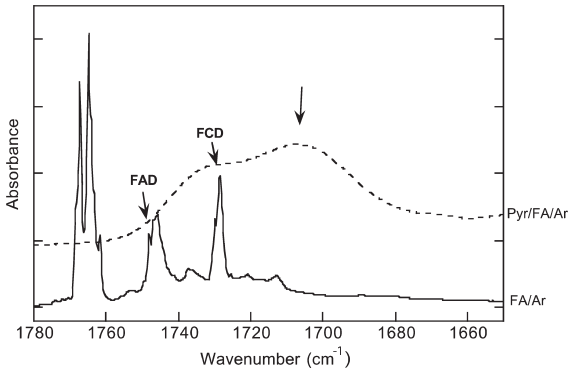

Figure 5. Infrared spectra in the C═O stretching region of FA at 16 K (after annealing) for a traditional matrix isolation experiment with FA/Pyr/Ar = 1/2/1000. The shifted C═O stretch is marked with an arrow. FAD indicates formic acid acyclic dimer; FCD indicates formic acid cyclic dimer.

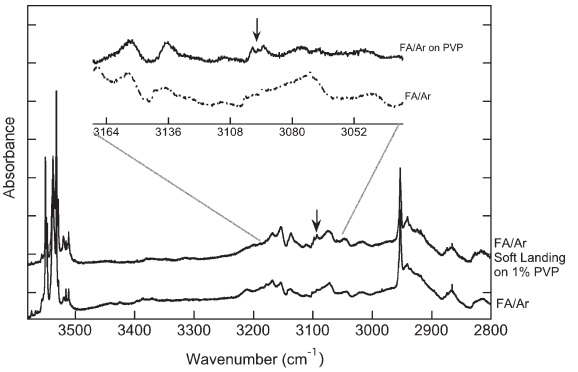

Figure 7. Infrared spectra in the O−H stretching region of FA at 16 K (after annealing) for Ar/FA = 250 (lower trace) and Ar/FA = 250 soft-landed on PVP. The expansion shows the result of subtraction of Ar/FA from Ar/FA on PVP. The shifted O−H stretch is marked with an arrow.

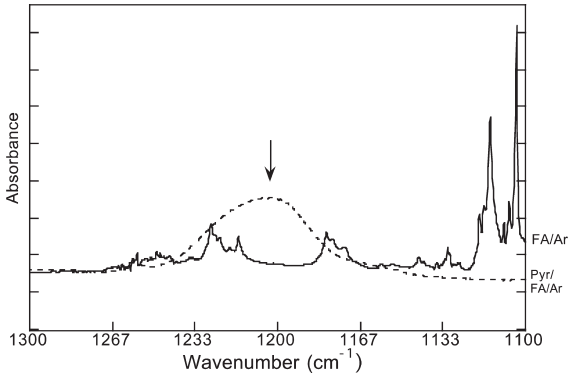

Figure 6. Infrared spectra in the C−O stretching region of FA at 16 K (after annealing) for a traditional matrix isolation experiment with FA/Pyr/Ar = 1/2/1000. The shifted C−O stretch is marked with an arrow.

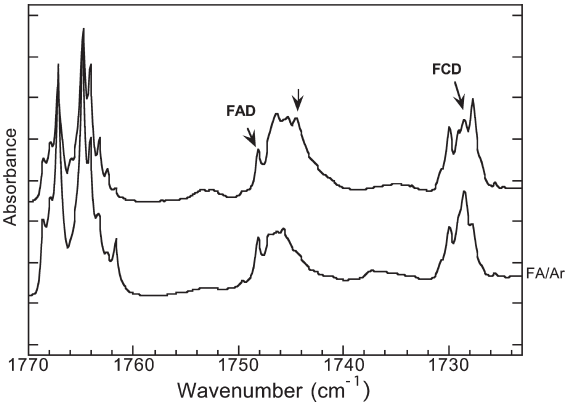

Figure 8. Infrared spectra in the C═O stretching region of FA at 16 K (after annealing) for Ar/FA = 250 (lower trace) and Ar/FA = 250 soft-landed on PVP. The shifted C═O stretch is marked with an arrow. FAD indicates formic acid acyclic dimer; FCD indicates formic acid cyclic dimer.

dx.doi.org/10.1021/jp2080012 |J. Phys. Chem. B 2012, 116, 211–220

FA−Pyr already exist,[9,13] we duplicated the FA−Pyr work just for comparison sake. We note that our results are in excellent agreement with the literature.

We also calculated frequencies for "dimer modes" for the PVP polymer (using two linked vinylpyridine monomers, as described in Experimental Methods) just to assess the effect of even a small polymer backbone (and acids in close proximity) on the behavior of the complex. We emphasize that the theoretical calculations are not the primary focus of this work especially because extensive theoretical work already exists for both FA and H_2O with Pyr and for Pccp with several other nitrogen bases. Selected calculated structures and relevant structural parameters are given in Figures S4 and S5 in Supporting Information.

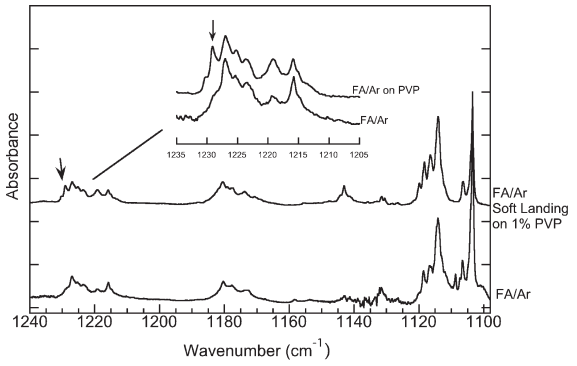

Figure 9. Infrared spectra in the C−O stretching region of FA at 16 K (after annealing) for Ar/FA = 250 (lower trace) and Ar/FA = 250 soft-landed on PVP. The upper spectrum shows an expanded view of both traces. The shifted C−O stretch is marked with an arrow.

DISCUSSION

Evidence for hydrogen bond formation between the acids and the pyridine ring comes from a direct comparison of the infrared spectra of the isolated acids (H_2O, FA, and Pccp) and bases (Pyr or PVP) (i.e., the blank or parent spectra) with those obtained in matrix isolation codeposition experiments and soft-landing experiments. For the three systems studied here, changes in hydrogen donor vibrational modes provide ample evidence for hydrogen bond formation and are also in excellent agreement with published work on these and similar systems.[8,9,11] Furthermore, in some cases changes in base modes were also observed. The details of each system will be described individually below.

H_2O + PVP. When H_2O/Ar was soft-landed on PVP, significant changes in two of the three characteristic vibrations of H_2O were observed. A red shift of 227.6 cm^{-1} in the symmetric O−H stretch (ν_1) appeared as an undergrowth to the red of water cluster bands (see Figure 1 panel A) and was visible and reproducible and able to be studied upon subtraction of the parent spectra (see Figure 1, panel B). We note, importantly, that we did not observe the parent symmetric O−H stretch (ν_1), likely because it falls within the envelope of the antisymmetric O−H stretch, and thus we calculated this shift based on the literature value[9] for this band. We thought this reasonable because our other two parent bands for H_2O agree within 2 cm^{-1} of the literature values (see Table 1). We acknowledge that this type of undergrowth as evidence for new product absorption is often difficult to pinpoint, but having a carefully selected *model system* such as water enabled us to know where to look for product bands. We note that water, although a good model system for us in some ways, also poses challenges in terms of the formation of clusters (dimers and trimers) and because the rotation of water monomers in an Ar matrix can give rise to

Table 1. Observed[a] and Calculated[b] Vibrational Frequencies for Key Modes of Acid−Pyridine (matrix isolation) and Acid−PVP (soft-landing) Complexes

ACID (matrix, parent)		ACID−pyridine (matrix)		ACID-PVP (soft-landing)		
exptl	(lit.[c]) calcd[d]	exptl (shift)	calcd (shift)	exptl (shift)	calcd (shift)	fundamental
H_2O		**H_2O−Pyr[c]**		**H_2O−PVP**		**H_2O mode**
3702.9	(3701), 3931.3	3701 (0)	3701 (0)	3702.9 (0)	3931.3(0)	ν_3 antisymmetric O−H stretch
3671[d]	(3671), 3809.2	3400 (−271)	3400 (−271)	3443.4 (−227.6)	3550.9 (−258.3)	ν_1 symmetric O−H stretch
1592.3	(1590), 1603.2	1616(+26)	1616(+26)	1612.3 (+20.0)	1635.8 (+32.6)	β_2 H−O−H bend
FA		**FA−Pyr**		**FA−PVP**		**FA mode**
3549.3[e]	3592.5	2902.3 (−647.0)	2812.5 (−780.0)	3095.7 (−453.6)	2799.1 (−793.4)	ν (O−H)
1767.2	1745.2	1707.4 (−59.8)	1698.8 (−46.4)	1744.4 (−22.8)	1695.7 (−49.5)	ν (C═O)
1103.6	1082.3	1203.4 (+99.8)	1182.0 (+99.7)	1229.1 (+125.5)	1185.2 (+102.9)	ν (C−O)
Pccp		**Pccp−Pyr**		**Pccp-PVP**		**Pccp mode**
3044.5	3192.8	2938.0 (−106.5)	3070.3 (−122.5)	2939.9 (−104.6)	3066.6 (−126.2)	ν_1 C−H stretch/a′
1295.6	1323.9	1348.4 (+52.8)	1363.5 (+39.6)	1360.3 (+64.7)	1370.9 (+47.0)	ν_2 C−H bend/a′
1204.5	1232.6	1229.3 (+24.8)	1244.3 (+11.7)	1215.5 (+11.0)	1252.5 (+19.9)	ν_3 ring/a′
1086.6	1108.6	1142.1 (+55.5)	1174.5 (+65.9)	1111.4 (+24.8)	1178.8 (+70.2)	ν_{13} C−H bend/a″
954.6	971.4	952.5 (−2.15)	969.6 (−1.8)	947.0 (−7.6)	969.9 (−1.5)	ν_{14} ring/a″
927.5	928.6	933.5 (+6.0)	925.4 (+3.2)	937.6 (+10.1)	931.4 (+2.8)	ν_4 ring/a′
897.8	887.1	895.4 (−2.4)	881.7 (−5.4)	888.4 (−9.4)	882.9 (−4.2)	ν_5 C−Cl stretch/a′

[a] Band positions in cm^{-1}. [b] Calculated (at the (B3LYP/6-31+G(d,p)) level. [c] Literature values, from ref 9, calculated at the (SCF/6-31++G(d,p)) level. The numbers in parentheses for parent H_2O/Ar matrix (column one) are the experimental parent H_2O/Ar values from ref 9. [d] Note well: We are using the literature value here from ref 9, as our band fell within the envelope of the v_3 band. [e] Multiplet; mean value reported.

dx.doi.org/10.1021/jp2080012 |J. Phys. Chem. B 2012, 116, 211–220

complicated band profiles.[19] We note that, in the O−H stretching region, dimers and trimers of water only appear above 3500 cm^{-1} and although the tails of those absorption bands may overlap with our new product absorption, we are confident that this new product is in fact the shifted O−H stretch, as it agrees well with the red shift of 271 cm^{-1} reported for the 1:1 H_2O−Pyr complex isolated in argon (see Table 1) and our spectra are strikingly similar to those obtained by Destexhe and co-workers.[9] It is well-known that this shift in ν_{OH} may be taken as a measure of the hydrogen bond strength.[19] Likewise, our blue shift of 20.0 cm^{-1} in the H−O−H bend (β_2) agrees will with the reported value of 26 cm^{-1} for matrix-isolated H_2O−Pyr. In this case, too, it was necessary to perform a subtraction to clearly observe the new product band at 1612.3 cm^{-1}, as a dimer band overlaps with our product band. Our product band is broad and intense, as we were depositing quite a concentrated sample of H_2O/Ar (1/200) compared to some matrix experiments with H_2O/Pyr/Ar at 1/1/2500. We knew we would have significant water clusters in our experiments, because even at the very dilute matrix conditions reported by Destexhe,[9] these clusters are still present. Again we note that the spectra obtained by Destexhe et al. in this region look exactly like ours in that they show a water dimer band and a product band for the 1:1 complex in exactly the same region. They rely only on an increase in intensity as evidence for a product band there and do not perform a subtraction but report their band to be at 1616 cm^{-1}, which agrees with their calculation exactly. Thus, we are confident that our product band at 1612.3 cm^{-1}, which does show up upon subtraction, does in fact correspond to the shifted O−H stretch, which on the PVP differs by only 4 cm^{-1} from the matrix result. We observed no shift in water's antisymmetric O−H stretch, a result also obtained in the matrix isolation experiments. Because the two main shifts we observe in our soft-landing experiments are in such good agreement with the matrix work, it is reasonable to conclude that we have in fact formed the same N···H_2O complex on the PVP polymer that forms with Pyr in an argon matrix.

Finally, we did observe blue shifts of 4.9 and 11.2 cm^{-1} for the ν (C−C) and the β (C−H) of the pyridine rings of the PVP, respectively. These same shifts have been reported by Maes[20] and theoretical calculations have been in good agreement.[21] Overall, our DFT calculations do, in fact, agree well with our observed shifts, with a difference between experiment and theory of 30.7 cm^{-1} in the symmetric O−H stretch and 12.6 cm^{-1} in the H−O−H bend.

Pccp + Base. For both the matrix and soft-landing experiments, product bands were observed over a wide range of reagent concentrations and matrix conditions. One advantage to this model system is that Pccp does not form dimers, and so we could work at higher concentrations (i.e., lower argon pressures in the line with the Pccp unrestricted). Another advantage is that Pccp, with five halogens and only one proton, has one site for hydrogen bond formation, and thus we are confident that we formed a 1:1 complex in both matrix and soft-landing experiments.

The matrix and soft-landing results are quite similar and are also strikingly similar to our published study on Pccp.[8] The observable most commonly used in the characterization of such hydrogen-bonded systems is the shift of the parent C−H stretch that involves the hydrogen-bonded hydrogen. Numerous studies involving alkynes[22] and alkenes[23] confirm that this shift, usually referred to as $\Delta\nu_s$ is a reliable measure of the strength of the interaction. We observed a red shift in Pccp's C−H stretch of 106.5 and 104.6 cm^{-1} in the matrix and soft-landing experiments, respectively (see Figure 3 and Table 1). These shifts are quite close to our value of 104.3 cm^{-1} for Pccp-NH_3, and we note a striking similarity between the spectra shown in Figure 3 and that of the Pccp-NH_3 complex, shown in Figure S1. In general, gas-phase basicities (i.e., proton affinities) govern the trend in ordering of $\Delta\nu_s$ in matrix work because there is no interference from a solvent. Our previous work demonstrates an ordering of $(CH_3)_2NH > (CH_3)NH_2 > NH_3 > CH_3CN$ with Pccp. Because the gas-phase basicity of Pyr is greater than that of $(CH_3)_2NH$[24] we expected to see a shift larger than our published value of 170.3 cm^{-1} for Pccp-$(CH_3)_2NH$. This is not true for Pyr in solution, and in fact the much lower basicity of Pyr compared to NH_3 and methylamines in solution is not only due to hybridization effects in Pyr but also (and more importantly) to solvation effects.[25] It is therefore interesting that in both matrix and soft-landing experiments where solvation effects should not be important, Pyr is demonstrating a reduced basicity, almost as if in solution. When H_2O was matrix-isolated with Pyr and pyrimidine (Pym), the strength of the hydrogen-bonded complexes did, in fact, reflect the differences in gas-phase basicities of Pyr and Pym.[9] Thus, we did not expect our anomaly. Our calculated hydrogen bond strength of 4.0 kcal/mol for Pccp−Pyr is equal to our published value for Pccp-NH_3.

In all experiments, additional modes of the Pccp were perturbed by hydrogen bond formation, as in our previous work. In particular, the ν_2C−H bending mode was blue-shifted by similar amounts (52.8 and 64.7 cm^{-1}) in the matrix and soft-landing experiments, respectively. Interestingly, the ν_{13}C−H bend and the ν_3 ring mode both shifted almost exactly twice as much in the matrix as compared to the soft-landing experiments (see Table 1). This is possibly due to a hindrance in the range of motion caused by the arrangement of the pyridine rings on the polymer as compared to the less hindered argon matrix alone.

In general, base modes were affected only slightly in the matrix experiments (all red shifts under 11 cm^{-1}) and in the soft-landing experiments ν_{C-C} in the pyridine rings blue-shifted by 15.5 cm^{-1}. It is interesting to note that many base ring modes were calculated to shift by large amounts but did not. We have seen this in past work, and perhaps the argon matrix as a cause for this hindrance in range of motion is more important here than any factors governed by the organized structure of the polymer.

FA + Base. When FA was either matrix-isolated with Pyr or soft-landed onto the PVP film, significant changes in the three main vibrations of FA were observed (see Table 1 and Figures 4−9). FA, like H_2O, is a good model system because the vibrational modes corresponding to the O−H, C═O, and C−O, which are key indicators of hydrogen bond formation, have been thoroughly studied in a matrix, in particular in studies involving FA−furan[26] and FA−acetylene[11,27] complexes. This is advantageous because FA suffers some of the same complications as does H_2O, namely persistent FA dimers that are always present, even at extremely low concentrations[11] and the splitting of parent bands because of site effects in the argon matrix.[28] The O−H stretching region (Figures 4 and 7) was straightforward to assign, both based on the published work[11] and the fact that there are no FA dimers in this region. The C═O region, however, contains a band at 1747.2 cm^{-1} for the acyclic FA dimer and one at 1728.0 cm^{-1} for the cyclic FA dimer (labeled as FAD and FCD, respectively, in Figures 5 and 8). Our dimer bands agree with the literature[29] exactly, and thus we are confident with our value for the C═O shift, which we carefully studied at a variety of

dx.doi.org/10.1021/jp2080012 |J. Phys. Chem. B 2012, 116, 211–220

concentrations. The matrix work proved to be quite difficult in terms of product formation. It is reported in the literature[11,26] that with mixtures of FA and base highly diluted in Ar, monomers of FA and base were the main products formed in the matrix, but upon annealing, the monomers diffuse, yielding a matrix that consists mainly of FA dimers and the desired complex between FA and the base. Sanchez-Garcia[26] demonstrated that at a ratio of FA/furan/Ar = 1/3/1500, FA parent bands are barely visible after annealing. We found that at a ratio of FA/Pyr/Ar = 1/2/1000, and after annealing, we did not observe parent bands (see Figures 4−6). It is notable that while product bands in our matrix spectra at these very dilute concentrations are broad, they are sharper and more well-defined in the soft-landing experiments at much higher concentrations (Ar/FA = 250, see Figures 7−9). Our product band in the C═O stretch region became much more distinct after annealing (see Figures 8 and S3). We also note that our DFT results, which agree extremely well with the published results,[13] also agree well with our experiment and were helpful in making assignments.

A very important result is that for FA, unlike H_2O and Pccp, there is a significant difference between the matrix isolation and soft-landing shifts in the three key vibrations of FA. In the matrix isolation experiments, a red shift of 647.0 cm^{-1} was observed for the O−H stretch of FA, whereas in the soft-landing experiments this red shift was 453.6 cm^{-1}, a difference of 193.4 cm^{-1}. Although FA and Pyr have never before been matrix-isolated, a detailed theoretical study on the hydrogen-bonding interaction between the two has been published,[13]and this study has been invaluable to us and has rendered FA a much more valuable model system than it would have been otherwise. Fernandez-Berridi and co-workers[13] identify five possible structures for the FA−Pyr complex. The most stable complex (structure 1) is calculated to have a red shift of 776 cm^{-1} in the O−H stretch, and the second most stable complex (structure 2) is calculated to have a red shift of 526 cm^{-1} (see Figure S6 in Supporting Information for structures 1 and 2 reproduced from reference 13). Interestingly, this difference of 250 cm^{-1} between the O−H shift in structure 1 versus structure 2 is in close agreement with our difference of 193.4 cm^{-1} between the matrix and soft-landing experiments. We also note that there is excellent agreement of absolute frequency values between our work and the theoretical study. No such similarities were seen with the additional and much less stable structures reported in the study. Another mode discussed in detail is FA's C═O stretch, which, in our matrix isolation experiments red-shifted by 59.8 cm^{-1} and by 22.8 cm^{-1} in the soft-landing experiments, yielding a difference of 37.0 cm^{-1} between the two techniques, which also agrees fairly well with the difference in shifts for this C═O stretch between structures 1 and 2, which is 59 cm^{-1}. Although the C−O stretching mode for FA is not discussed in the theoretical study, we observe a blue shift of 99.8 and 125.5 cm^{-1} in the matrix and soft-landing experiments, respectively. This comparison provides quite reasonable evidence that we in fact have matrix-isolated a FA−Pyr complex quite like structure 1 but have formed a FA−Pyr complex similar to structure 2 on the pyridine rings attached to the polymer backbone of PVP. We also note that our shifts in the matrix experiments agree well with those for the acetic acid−Pyr complex.[25] Structure 1, which has a binding energy of 11.1 kcal/mol, is characterized by two hydrogen-bonding interactions, namely O−H···N (usually written as N···H−O) and C═O···H−C (usually written as C−H···O, but we prefer to show the C═O functional group for clarity). These two cooperative interactions require FA and Pyr to orient parallel to each other on the same molecular plane, which maximizes the interaction between the N and the O−H and also makes it possible for the second interaction between the α C−H of the Pyr and the carboxylic oxygen of FA. In structure 2, which has a binding energy of 6.16 kcal/mol, the FA and Pyr are not in the same plane but rather lie in planes perpendicular to each other, and the α C−H···O (or C═O···H−C) hydrogen-bonding interaction is absent. This orientation causes a lengthening of the N···H distance from 1.72 Å in structure 1 to 1.77 Å in structure 2 (Figure S6). Although questions remain about the exact nature of the PVP structure, it has been shown[10] that after adsorption of PVP onto a surface such as glass or CaF_2, PVP molecules will have numerous unbound pyridyl groups that do not participate in the interaction with the surface and are therefore capable of interacting with molecules such as those studied here, or nanoparticles. The pyridine rings are not uniform; some are parallel to the surface and some are somewhat slanted, but the rings are not perpendicular to the surface. One study reports that, under certain conditions, the pyridine rings have a tilt angle of about 45° in the plane perpendicular to the backbone.[30] Therefore, it is likely that there is not enough room in between pyridine rings on the PVP for the FA to lie in the same plane as the ring. Thus, the main hydrogen bonding interaction is the O−H···N in which structure 2 takes part. The argon matrix, on the other hand, allows for FA and Pyr to lie in the same plane, as in structure 1.

Finally, we note that in the FA−Pyr matrix isolation experiments, we observe blue shifts in three modes associated with C−H stretches of the Pyr rings (see Figure 4) whereas in the soft-landing experiments, we do not observe any changes at all in vibrational modes associated with the PVP. These significant shifts of 50.5, 62.1, and 66.1 cm^{-1} provide further evidence for the conclusion we draw above, namely that the FA is more strongly bound to the Pyr ring in the matrix (with two hydrogen-bonding interactions) as compared to the PVP.

Although it was not the intent of this work to focus on theoretical details, we do feel that some points are of interest. Notably, the calculated structures of both H_2O−PVP and FA−PVP (shown in Figures S4 and S5) show that the bond angles and lengths are not equal for the acids on adjacent vinylpyridine units. This is interesting in light of the fact that our method of modeling these systems (i.e., modeling only two monomer units of the PVP polymer) is quite limiting in that it excludes having an acid molecule in the center of two others and also excludes this same type of interaction linked monomers. This in turn eliminates a close look at the cooperative effects involved in the hydrogen bonding in these systems. Despite this, it is still the case that each acid molecule has a slightly different structure and behaves as if in a different "site". Additional modeling of a larger portion of the polymer has the potential to elucidate important structural information about the polymer structure and its effect on hydrogen bonding, and we plan to pursue such studies.

The matrix isolation technique has several advantages over other methods for characterizing hydrogen-bonded complexes. One such advantage is that samples may be deposited for long periods of time (24 h is not unusual) to ensure a large path length for absorption in accordance with Beer's Law and thus product bands of adequate intensity in the infrared spectrum. In soft-landing studies,[6] however, much less material is deposited, and thus the sample to be analyzed is very thin. This poses spectral challenges in terms of sensitivity and resolution. Soft-landing studies typically employ infrared reflection absorption spectroscopy

(IRAS) to probe the structure of the complexes formed. This method has been shown to provide some advantages over absorption alone and is also often necessary because most soft-landing substrates are opaque metals such as gold and silicon.[6] The work presented here demonstrates that we do in fact have enough hydrogen-bonded product on the PVP polymer to be successful with FTIR absorption spectroscopy, under the same conditions as a traditional matrix isolation experiment. We performed experiments on a range of PVP solution concentrations and were most successful with a 1% solution, which has been shown to yield the highest number of available sites for hydrogen bond formation.[10] Although our plots do not show absorbance units (for ease of comparing two very different scales), we were able in all soft-landing experiments to obtain enough hydrogen-bonded product to yield an infrared spectrum with an adequate signal and all of the necessary spectral features for successful analysis at 0.5 cm^{-1} resolution and with 32 scans (as compared to 500 scans in most soft-landing experiments). In fact, for our soft-landing experiments, typical product absorbance values were in the range 0.01−0.3, as compared to 0.3−1.0 for the matrix isolation experiments. In addition, our absorbance values are often larger than those reported,[6] many of which are between 0.003 and 0.008, and less than 0.2% transmittance, if reported this way. Even in the case of small absorbance values, however, spectral features were clear and distinct, and in several cases spectral subtraction further confirmed the location of product bands.

Finally, the aspect of time has emerged as an interesting aspect of this work. An examination of our experiment progress over time (see Figures S2 and S3) demonstrates that the sites available for hydrogen bond formation are not occupied within a few seconds, or even minutes. This is quite surprising, as the rate of growth of matrix thickness has been shown to be approximately 8−10 μm per hour at flow rates we have employed.[15] This means that all of the possible sites for hydrogen bond formation *on the surface of the polymer* are occupied in seconds, and after that the parent molecules (along with aggregates as applicable) and argon are building up in excess on the surface. Although for FA it is difficult to tell exactly when maximum amount of product was achieved because of overlapping bands, it appears that the product band at 1744.4 cm^{-1} (C═O stretch) is the most distinct after 4.5 h, and prior to 1 h, there are no clear spectral features. After annealing, however, this product band grows in intensity (see Figure S3), which means that parent molecules were still able to find unoccupied sites for hydrogen bonding. For Pccp, where there is no interference from parent bands, it appears that the soft-landing experiment was over in 17 min and annealing did not produce additional product (see Figure S2). Since, in general, we continue to observe product formation for minutes and possibly even hours, we must conclude that hydrogen bonding is taking place *both on and beneath* the surface of the polymer. It has been shown in the soft-landing experiments reported in the literature[6] that molecules can penetrate the argon to some extent, and thus if this were happening in our experiments, that mechanism could provide us with additional parent molecules reaching the polymer surface, but we estimate that this effect, too, would terminate within seconds. The only plausible explanation for product formation over minutes to hours is that parent molecules are diffusing into the polymer, and in fact this process is occurring independently of further deposition. Thus, we continue to build up excess parents on the surface that will never make it to hydrogen-bonding sites, but the parent molecules that reached the polymer within those initial seconds continue to move through the polymer to find hydrogen-bonding sites over time, until all sites are occupied. Annealing can have the effect of further increasing movement of parent molecules through the polymer. Polymer studies reported in the literature have in fact shown that diffusion of small molecules through polymers is a common and important transport phenomenon.[31] Although transport properties depend on many factors, the two that seem relevant here are "free volume within the polymer and segmental mobility of the polymer chains".[31] While free volume varies from polymer to polymer, the constant motion of the polymer (especially at room temperature) can cause the free volume (as well as the shapes of the available channels) to change rapidly, sometimes blocking off available pathways. At the very low temperatures we employ, the polymer is rigid and thus the chain mobility decreases considerably. While the polymer is in a more "fixed" form, small molecules can move through open networks within the polymer and continue to find sites on which to hydrogen bond. Equally important is the fact that at low temperatures, our parent molecules are diffusing slowly, and this *slow diffusion combined with the increased amount of free volume within the polymer* results in the continuation of the experiment until a saturation point occurs. This phenomenon adds an interesting dimension to this work, namely that future experiments will enable us to use small molecules as a probe for investigating the relationship between polymer structure and transport properties by varying conditions such as temperature and extent of annealing.

CONCLUSIONS

Hydrogen-bonded complexes of H_2O−Pyr, Pccp−Pyr, and FA−Pyr were formed both in an argon matrix at 16 K when the acids and Pyr were codeposited in a traditional matrix isolation experiment and when the acids, diluted in argon, were deposited onto the PVP surface also at 16 K. In all experiments, significant changes in vibrational modes of the proton donor species provided firm evidence for hydrogen bond formation. Unlike all previous work coming from our laboratory, this study focuses on hydrogen-bonded complexes that are already fairly well understood so that they would serve as good model systems for a comparative study of two slightly different techniques. This work represents the first such detailed comparison of two techniques and, more specifically, the first comparison of an isolated base such as pyridine with the pyridine ring (i.e., pyridyl functional group) on the PVP polymer. The overall similarity of the matrix and polymer soft-landing results to each other and to the literature demonstrates that there is certainly hydrogen bond formation between the three acids studied and the pyridine "functional group". In the case of H_2O and Pccp, where there is one possible site for hydrogen bond formation (i.e., the "acidic" proton with the N of the base to form O−H···N and C−H···N linkages, respectively), very similar complexes form in the argon matrix as on the PVP polymer. In the case of FA, however, where several possibilities for hydrogen bond formation have been documented, two different complexes form (see Figure S6). In the argon matrix, the FA−Pyr complex is bound by two hydrogen-bonding interactions: one between the hydroxyl proton of FA to form an O−H···N linkage, and a second between the carbonyl oxygen of FA and the α hydrogen on the pyridine ring to form a C═O···H−C linkage. This result is quite significant in that it demonstrates that the PVP backbone and arrangement of the pyridine rings on the PVP polymer plays a

role in fixing the geometry of the FA—Pyr complex. This, in turn, means that the two techniques can also serve, in a comparative way, to probe the effect of the polymer on the complex. The complex on the PVP has only one hydrogen-bonding interaction, namely the O—H···N, quite likely because there is not enough room for FA and Pyr to lie parallel in the same plane. Since they are forced to be perpendicular, the possibility for the secondary hydrogen-bonding interaction is eliminated. We realize that the existing detailed theoretical study of FA—Pyr complexes helped us to draw this conclusion, and in future work the use of DFT to predict possible structures will be essential.

Finally, the matrix isolation community has for a long time been supplying important structural information via isolated, model systems to fields such as atmospheric and environmental chemistry. This work demonstrates the ability of the matrix and polymer soft-landing isolation techniques to provide valuable information regarding hydrogen bonding to those in the field of nanochemistry, thus aiding in the design of nanostructures.

■ ASSOCIATED CONTENT

Supporting Information. Our previously published spectrum of Pccp/Ar parent with Pccp/NH_3/Ar is reproduced in Figure S1. Spectra showing the progress of the soft-landing experiments over time for both Pccp and FA are shown in Figures S2 and S3, respectively. Geometries of selected calculated structures (Pccp—Pyr, Pccp-PVP, FA—Pyr, and FA—PVP) are shown in Figures S4 and S5. In Figure S6, the two important structures for FA—Pyr are reproduced from reference 13. This material is available free of charge via the Internet at http://pubs.acs.org.

■ AUTHOR INFORMATION

Corresponding Author

*Phone: 717-245-1295. Fax: 717-245-1995. E-mail: samet@dickinson.edu.

■ ACKNOWLEDGMENT

We gratefully acknowledge support of a portion of this research by a student—faculty summer research grant from Dickinson College. We especially thank Dickinson College for the outstanding new Rector Science Complex, in which all of this research was conducted.

■ REFERENCES

(1) Scaccianoce, L.; Braga, D.; Calhorda, M. J.; Grepioni, F.; Johnson, B. F. G. *Organometallics* **2000**, *19*, 790–797.
(2) Chao, M. H.; Kumaresan, S.; Wen, Y. S.; Lin, S. C.; Hwu, J. R.; Lu, K. L. *Organometallics* **2000**, *19*, 714–717.
(3) Hansen, J. G.; Feeder, N.; Hamilton, D. G.; Gunter, M. J.; Becher, J.; Sanders, J. K. M. *Org. Lett.* **2000**, *2*, 449–452.
(4) Ariga, K.; Hill, J. P.; Ji, Q. *Phys. Chem. Chem. Phys.* **2007**, *9*, 2319–2340 and references therein.
(5) Stockton, W. B.; Rubner, M. F. *Macromolecules* **1997**, *30*, 2717–2725.
(6) Nagaoka, S.; Matsumoto, T.; Okada, E.; Mitsui, M.; Nakajima, A. *J. Phys. Chem. B* **2006**, *110*, 16008.
(7) Bedell, B. L.; Goldfarb, L.; Mysak, E. R.; Samet, C.; Maynard, A. *J. Phys. Chem. A* **1999**, *103*, 4572–4579.
(8) Baker, A. B.; Samet, C.; Lyon, J. T.; Andrews, L. *J. Phys. Chem. A* **2005**, *109*, 8280–8289.
(9) Destexhe, A.; Smets, J.; Adamowicz, L.; Maes, G. *J. Phys. Chem.* **1994**, *98*, 1506–1514.
(10) Malynych, S.; Luzinov, I.; Chumanov, G. *J. Phys. Chem. B* **2002**, *106*, 1280–1285.
(11) George, L.; Sanchez-Garcia, E.; Sander, W. *J. Phys. Chem. A* **2003**, *107*, 6850–6858.
(12) Marushkevich, K.; Siltanen, M.; Rasanen, M.; Halonen, L.; Khriachtchev, L. *J. Phys. Chem. Lett.* **2011**, *2*, 695–699.
(13) Fernandez-Berridi, M.; Iruin, J. J.; Irusta, L.; Mercero, J. M.; Ugalde, J. M. *J. Phys. Chem. A* **2002**, *106*, 4187–4191.
(14) Wang, L. Y.; Fu, Y.; Wang, Z. Q.; Fan, Y. G.; Zhang, X. *Langmuir* **1999**, *15*, 1360–1363.
(15) Dunkin, I. R. In *Matrix-Isolation Techniques: A Practical Approach*; Oxford University Press: New York, 1988.
(16) Armarego, W. L. F.; Chai, C. L. L. In *Purification of Laboratory Chemicals*; Butterworth-Heinemann: Burlington, MA, 2009.
(17) Frisch, M. J.; Trucks, G. W.; Schlegel, H. B.; Scuseria, G. E.; Robb, M. A.; Cheeseman, J. R.; Montgomery, Jr., J. A.; Vreven, T.; Kudin, K. N.; Burant, J. C.; Millam, J. M.; Iyengar, S. S.; Tomasi, J.; Barone, V.; Mennucci, B.; Cossi, M.; Scalmani, G.; Rega, N.; Petersson, G. A.; Nakatsuji, H.; Hada, M.; Ehara, M.; Toyota, K.; Fukuda, R.; Hasegawa, J.; Ishida, M.; Nakajima, T.; Honda, Y.; Kitao, O.; Nakai, H.; Klene, M.; Li, X.; Knox, J. E.; Hratchian, H. P.; Cross, J. B.; Bakken, V.; Adamo, C.; Jaramillo, J.; Gomperts, R.; Stratmann, R. E.; Yazyev, O.; Austin, A. J.; Cammi, R.; Pomelli, C.; Ochterski, J. W.; Ayala, P. Y.; Morokuma, K.; Voth, G. A.; Salvador, P.; Dannenberg, J. J.; Zakrzewski, V. G.; Dapprich, S.; Daniels, A. D.; Strain, M. C.; Farkas, O.; Malick, D. K.; Rabuck, A. D.; Raghavachari, K.; Foresman, J. B.; Ortiz, J. V.; Cui, Q.; Baboul, A. G.; Clifford, S.; Cioslowski, J.; Stefanov, B. B.; Liu, G.; Liashenko, A.; Piskorz, P.; Komaromi, I.; Martin, R. L.; Fox, D. J.; Keith, T.; Al-Laham, M. A.; Peng, C. Y.; Nanayakkara, A.; Challacombe, M.; Gill, P. M. W.; Johnson, B.; Chen, W.; Wong, M. W.; Gonzalez, C.; Pople, J. A. *Gaussian 03, Revision C.02*; Gaussian, Inc., Wallingford, CT, 2004.
(18) Hao, E. C.; Lian, T. Q. *Langmuir* **2000**, *16*, 7879–7881.
(19) Engdahl, A.; Nelander, B. *J. Mol. Struct.* **1989**, *193*, 201.
(20) Maes, G.; Smets, J. *J. Mol. Struct.* **1992**, *270*, 141.
(21) Del Bene, J. E. *J. Am. Chem. Soc.* **1975**, *97*, 5330–5335.
(22) DeLaat, A. M.; Ault, B. S. *J. Am. Chem. Soc.* **1987**, *109*, 4232–4236.
(23) Jeng, M. L. H.; Ault, B. S. *J. Phys. Chem.* **1990**, *94*, 4851–4855.
(24) Dzidic, I. *J. Am. Chem. Soc.* **1972**, *94*, 8333–8335.
(25) Remko, M. *Adv. Mol. Relax. Interact. Processes* **1980**, *16*, 155.
(26) Sanchez-Garcia, E.; Mardyukov, A.; Studentkowski, M.; Montero, L. A.; Sander, W. *J. Phys. Chem. A* **2006**, *110*, 13775–13785.
(27) Sanchez-Garcia, E.; George, L.; Montero, L. A.; Sander, W. *J. Phys. Chem. A* **2004**, *108*, 11846–11854.
(28) Ito, F. *J. Chem. Phys.* **2008**, *128*, 114310.
(29) Marushkevich, K.; Khriachtchev, L.; Lundell, J.; Domanskaya, A.; Rasanen, M. *J. Phys. Chem. A* **2010**, *114*, 3495–3502.
(30) Lee, S. W.; Chae, B.; Hahm, S. G.; Lee, B.; Kim, S. B.; Ree, M. *Polymer* **2005**, *46*, 4068.
(31) George, S. C.; Thomas, S. *Prog. Polym. Sci.* **2001**, *26*, 985–1017.